

## Evaluation of (2-Hydroxyethyl) Triphenyl Phosphonium Bromide as Corrosion Inhibitor for Mild Steel in Sulphuric Acid

Hemlata Vashisht<sup>1</sup>, Sudershan Kumar<sup>1,\*</sup>, Indra Bahadur<sup>2</sup>, Gurmeet Singh<sup>1</sup>

<sup>1</sup>Department of Chemistry, University of Delhi, Delhi-110007

<sup>2</sup>Thermodynamics Research Unit, School of Engineering, University of KwaZulu-Natal, Howard College Campus, King George V Avenue, Durban, 4041, South Africa

\*E-mail: [sudershankumar2005@gmail.com](mailto:sudershankumar2005@gmail.com)

Received: 1 September 2013 / Accepted: 13 October 2013 / Published: 8 December 2013

---

The inhibition effect of the (2-Hydroxyethyl) triphenyl phosphonium bromide (HETPB) on mild steel corrosion in 0.5 M H<sub>2</sub>SO<sub>4</sub> have been determined by electrochemical techniques like potentiodynamic polarization (PDP), potentiostatic polarization (PSP) and electrochemical impedance spectroscopy studies (EIS). Potentiodynamic polarization study reveal that HETPB is an anodic type inhibitor with 98% efficiency at the concentration range of (1×10<sup>-2</sup> to 4×10<sup>-3</sup>) M for mild steel in 0.5 M sulfuric acid. Potentiostatic polarization study shows that HETPB is a non-passivating type of inhibitor at higher concentrations and act as passivating type of inhibitor at lower concentrations. The corrosion behavior of steel in 0.5 M H<sub>2</sub>SO<sub>4</sub> without and with the inhibitor at various concentrations was studied at the temperature range of (298 to 328) K. The adsorption of HETPB accords to Langmuir adsorption isotherm. Kinetic parameter such as effective activation energy (E<sub>a</sub>) has been evaluated from the effect of temperature on corrosion and inhibition processes. The negative values of thermodynamic parameter like Gibbs free energy of adsorption (ΔG<sup>o</sup><sub>ads</sub>) indicate the spontaneity of adsorption process. The surface morphology of the tested mild steel specimens in the presence and absence of inhibitors have been studied by using the respective images of SEM and AFM. Quantum chemical calculations have been performed and several quantum chemical indices were calculated and correlated with the corresponding inhibition efficiencies.

---

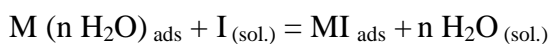
**Keywords:** Phosphonium compound; Corrosion inhibitors; Mild steel; Adsorption isotherms; Sulfuric acid solution

### 1. INTRODUCTION

Organic and inorganic compounds are widely used as corrosion inhibitors to control the corrosion [1-13]. Corrosion inhibition of mild steel is a matter of theoretical as well as practical importance [14]. Mild Steel is an extensively used metal in the industries, especially for structural applications, but it has high rate of dissolution in acidic medium, which is a major obstacle in its use

on a large scale. Acids are widely used in industries such as pickling, cleaning, and descaling. Since the acids are highly aggressive, inhibitors are used to reduce the rate of dissolution of metals [15-19]. Use of corrosion inhibitors is one of the best methods to control the corrosion in acidic medium. Corrosion process in metals can be controlled by treating them in solutions of special compounds which would be able to interact with the metal and thus their surface gets modified. For this type of surface modification the most efficient inhibitors are organic compounds with a molecular structure of  $\pi$ -conjugation.

The efficiency of an organic compound, to act as a corrosion inhibitor, depends on its ability to adsorb and interact with metal atoms through their heteroatom. Compounds containing nitrogen, sulphur, and oxygen have been reported as inhibitors [20-25]. The basic action of inhibitor is attributed to an increase in ohmic resistance of an inhibitor film at the electrolyte interface or due to some type of adsorption on the metal surface. Adsorption of inhibitor on the metal-solution interface is accompanied by a change in potential difference between the metal electrode and the solution due to the non-uniform distribution of electric charges at the interface. When an organic compound is used as a corrosion inhibitor, it is adsorbed at the metal-solution interface, and can be represented as:



A large number of phosphonium compounds are known to be applicable as corrosion inhibitors for mild steel. Phosphonium compounds exhibit surface-active properties; reduce foaming which often is a problem in water systems. They improve the corrosion resistance of metals and can be applied on the substrate by immersion or by incorporating it in a polymer coating system. Further, the existing literature revealed that no single inhibitor exhibited 100% corrosion inhibition efficiency. There is always a great demand for developing such efficient inhibitors for controlling the corrosion process. The objective of the present work is to focus on the inhibition action of HETPB on the corrosion of mild steel in 0.5 M  $H_2SO_4$  at (298 to 328) K. The work is carried out to establish the effective concentration for good inhibition action. The inhibition efficiencies of these compounds are determined by polarization and impedance methods. The surface morphology study is undertaken to establish good corrosion protection of HETPB.

## 2. EXPERIMENTAL

### 2.1. Inhibitor Used

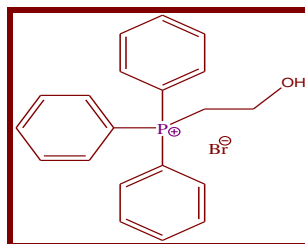


**Figure 1.** Molecular structure of HETPB.

The organic additive (2-Hydroxyethyl) triphenyl phosphonium Bromide,  $\text{HOCH}_2\text{CH}_2\text{P}(\text{C}_6\text{H}_5)_3\text{Br}$  used in this work are given in Figure 1 as the inhibitor has the following physical properties such as M.W. = 389.27g, Assay = 97% and M.P = 217-219 °C.

## 2.2. Electrodes and Chemicals

The working electrodes used in this experiment were prepared from a mild steel rod with the chemical compositions of (wt %): C (0.15), Si (0.31), S (0.025), P (0.025), Mn (1.02) and Fe (balance). The working electrode (WE) for the polarization and electrochemical impedance studies, was cut from mild steel rod and was soldered on one end with an insulated copper wire and it was then embedded in chemical epoxy resin (ARALDITE) leaving the exposed surface area of 1 cm<sup>2</sup> for the studies. Electrochemical experiments were performed in a conventional three electrode electrochemical cell with mild steel as a working electrode, a platinum counter electrode and saturated calomel electrode (SCE) as a reference electrode was coupled to luggin capillary. A steady state potential was achieved in 4-5 hours by immersing the working electrode into the test solutions. Prior to all measurements, the mild steel coupons were grounded with different empery papers (grade 100, 150, 320, 400, 600, 1000 and 1500) rinsed with double distilled water, degreased with acetone and dried at room temperature before being used. Properly grinded and polished samples of mild steel (0.5cm x 0.5cm x 0.5cm) were used for SEM and AFM. The aggressive solution (0.5 M H<sub>2</sub>SO<sub>4</sub>) was made by dilution of analytical grade 98% with double distilled water. The concentration range of employed inhibitor was ( $1 \times 10^{-2}$  to  $1 \times 10^{-3}$ ) M in 0.5 M sulfuric acid.

## 2.3. Electrochemical measurements

Potentiodynamic Polarization (PDP) and Potentiostatic Polarization (PSP) measurements were performed using electrochemical analyzer CHI 6021B under aerated conditions. The electrode system used for potentiostatic polarization studies and electrochemical impedance spectroscopy were same as the one used for PDP studies. Potentiodynamic anodic and cathodic polarization curves were obtained with a scan rate of 0.001Vs<sup>-1</sup> in the potential range from (-1.0 to 0.0) V relative to the corrosion potential ( $E_{\text{corr}}$ ). PSP curves were obtained with a scan rate of 0.01Vs<sup>-1</sup> in the potential range from open circuit potential (OCP) to 2 V. Electrochemical impedance spectroscopy was performed using electrochemical analyzer CHI 760C under aerated conditions. Impedance spectra were recorded at  $E_{\text{corr}}$  in the frequency range 10000Hz to 1Hz. The AC voltage amplitude was 0.005 V.

## 2.4. Surface Morphological Studies

After being immersed in 0.5 M H<sub>2</sub>SO<sub>4</sub>,  $1 \times 10^{-2}$  M HETPB and  $1 \times 10^{-3}$  M HETPB of the inhibitor in 0.5 M H<sub>2</sub>SO<sub>4</sub> for 24 hours at room temperature, the sample was taken out of the solutions and dried in desiccator for 24 hours and then these samples were used for SEM and AFM. SEM measurements were performed using Leo 435 VP in high vacuum mode and equipped with digital imaging and 35mm

photography system. SEM images were obtained by applying operative voltage of (15-30) KV. AFM measurements were performed using VEECO CPII atomic force microscope model no. MPP-11123 using resonance frequency  $f_0 = 20-80\text{N/m}$  and spring constant  $k = 20-80\text{N/m}$ . The topographic images were measured by AFM applying force in nano newton between the sample and Al- coated conductive tip.

### 2.5. Quantum Chemical Calculations

Quantum chemical analysis was performed using the PM3 method of the quantum chemical package MOPAC 6.0 of Hyperchem 7.5. The following quantum chemical indices were taken into consideration: the energy of the highest occupied molecular orbital ( $E_{\text{HOMO}}$ ), the energy of the Lowest unoccupied molecular orbital ( $E_{\text{LUMO}}$ ), energy band gap,  $\Delta E = E_{\text{HOMO}} - E_{\text{LUMO}}$ , binding energy, heat of formation and the dipole moment ( $\mu$ ).

## 3. RESULTS AND DISCUSSION

### 3.1. Potentiodynamic Polarization Studies

Figure 2(a) and 2(b) presents polarization curves for mild steel in 0.5 M  $\text{H}_2\text{SO}_4$  at four different temperatures i.e. at (298, 308, 318 and 328) K, in the absence and the presence of phosphonium compound at various concentrations ( $1 \times 10^{-2}$ ,  $7 \times 10^{-3}$ ,  $4 \times 10^{-3}$  and  $1 \times 10^{-3}$ ) M.

Electrochemical corrosion parameters, such as corrosion potential ( $E_{\text{corr}}$ ), cathodic and anodic Tafel slopes ( $b_a$  and  $b_c$ ) and corrosion current ( $i_{\text{corr}}$ ), obtained by extrapolation of the Tafel lines, are given in Table 1.

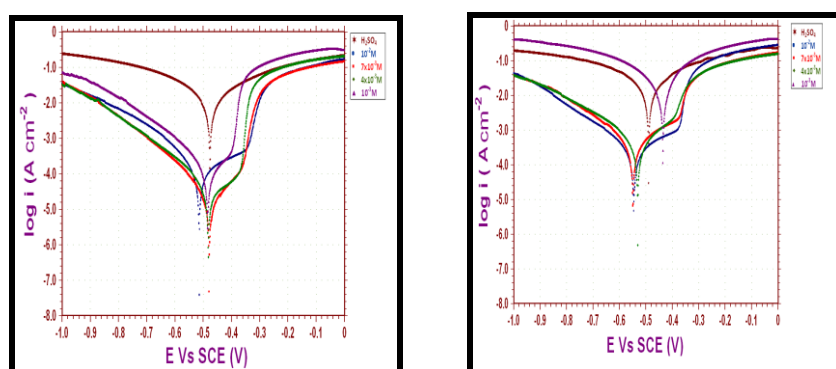


**Figure 2.** Anodic and cathodic polarization curves for mild steel at 298 K (a) and 328 K (b) in 0.5 M  $\text{H}_2\text{SO}_4$  in various concentrations of HETPB.

**Table 1.** Corrosion parameters such as corrosion potential ( $E_{\text{corr}}$ ), cathodic and anodic tafel slopes ( $b_c$  and  $b_a$ ), corrosion current ( $i_{\text{corr}}$ ) and inhibition efficiency ( $I\%$ ) of mild steel in 0.5 M  $\text{H}_2\text{SO}_4$  in the presence of HETPB at different temperatures.

TEMP. (K)	CONC. (M)	$-E_{\text{corr}}$ (V)	$b_c$ (mV/dec)	$b_a$ (mV/dec)	$i_{\text{corr}}$ ( $\text{A}/\text{cm}^2$ ) $\times 10^5$	$I\%$
<b>298</b>	$10^{-2}$	0.513	7.397	3.811	14.55	98.84
	$7 \times 10^{-3}$	0.478	7.755	12.113	1.19	99.98
	$4 \times 10^{-3}$	0.481	6.563	13.118	1.49	99.97
	$10^{-3}$	0.459	8.419	12.756	2.54	99.96
	$\text{H}_2\text{SO}_4$	0.464	5.302	6.659	967.90	
<b>308</b>	$10^{-2}$	0.492	7.611	17.200	2.62	99.85
	$7 \times 10^{-3}$	0.529	6.894	4.124	29.07	98.30
	$4 \times 10^{-3}$	0.516	6.601	5.679	28.93	98.31
	$10^{-3}$	0.484	7.070	13.258	5.17	99.69
	$\text{H}_2\text{SO}_4$	0.474	4.452	5.361	1712.00	
<b>318</b>	$10^{-2}$	0.565	6.453	4.540	21.93	98.88
	$7 \times 10^{-3}$	0.512	6.146	12.790	10.12	99.48
	$4 \times 10^{-3}$	0.535	6.044	5.569	35.13	98.20
	$10^{-3}$	0.454	5.318	7.531	567.30	70.97
	$\text{H}_2\text{SO}_4$	0.480	4.074	4.224	1954.00	
<b>328</b>	$10^{-2}$	0.545	5.647	3.784	33.57	98.48
	$7 \times 10^{-3}$	0.548	5.589	4.409	47.81	97.83
	$4 \times 10^{-3}$	0.530	5.524	7.608	39.99	98.12
	$10^{-3}$	0.435	5.006	4.918	2022.00	8.46
	$\text{H}_2\text{SO}_4$	0.489	3.889	4.781	2209.00	

The inhibition efficiency was calculated by using the following expression given below:

$$I\% = \left( \frac{i_o - i}{i_o} \right) \times 100 \quad (1)$$

where  $i_o$  is the corrosion current in the uninhibited solution and  $i$  is the corrosion current in the inhibited solution. The obtained values of inhibition efficiency ( $I\%$ ) are given in Table 1. These results show that HETPB acts as an effective inhibitor for corrosion of mild steel in 0.5 M  $\text{H}_2\text{SO}_4$ . The corrosion current values are much lower in the presence of the inhibitor than in pure acid. This shows that the inhibition is due to the adsorption of the additive on the mild steel surface. This was mainly due to the blocking effect of the surface by film formation which reduces the corrosion rate by the attack of acid environment. This achievement exhibited by the hetero atom, phosphorous atom, halogen atom (bromide) and olefinic bonds present in the inhibitor. These results show that inhibition efficiency of HETPB is greater than butyl triphenyl phosphonium bromide BuTPPB, 4-vinylbenzyl triphenyl phosphonium chloride VTPC, Cetyl Trimethyl Ammonium Bromide (CTAB) and 2-butyl-hexahydropyrrolo[1,2-b][1,2]oxazole BPOX [26-29].

The inhibition efficiencies is obtained (99 to 98) % for ( $1 \times 10^{-2}$  to  $4 \times 10^{-3}$ ) M HETPB up to 328 K but for lower concentration, which is  $1 \times 10^{-3}$  M shows 98 % inhibition efficiency up to 308 K,

there is significant drop of inhibition efficiency (70 to 8) % at (318 to 328) K temperatures. This might be due to the breaking of film formation at higher temperature.

The values of  $b_c$  and  $b_a$  shows irregular trend indicating the involvement of other species/anions present in the solution in the adsorption process.  $E_{corr}$  remains constant indicating that HETPB is a mixed type of inhibitor i.e. blocks both cathodic and anodic reactions to an equal extent. As  $b_a$  values are greater than  $b_c$  values which indicates that corrosion process is taking place by blocking anodic dissolution process. This indicates that HETPB predominantly act as anodic type of inhibitor.

### 3.2. Potentiostatic Polarizations Studies

The steady state potentiostatic behavior of the anodic dissolution of mild steel in 0.5 M  $H_2SO_4$  in the absence and in the presence of HETPB was studied and given in Figure 3.

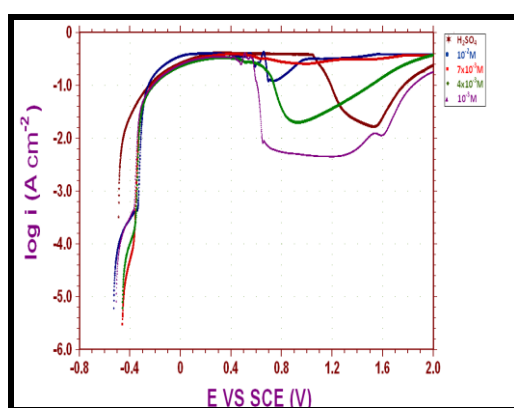


**Figure 3.** Potentiostatic polarization curves obtain for mild steel at 298 K in 0.5 M  $H_2SO_4$  in the various concentrations of HETPB.

From the typical potentiostatic polarization curves, the various parameters ( $i_c$  and  $i_p$ ) were determined and are given in Table 2.

**Table 2.** Electrochemical parameters ( $i_c$  and  $i_p$ ) for anodic dissolution of mild steel in 0.5 M  $H_2SO_4$  in the presence of HETPB.

Solutions	Concentration (M)	$i_c$ (A/cm <sup>2</sup> )	$i_p$ (A/cm <sup>2</sup> )	$E_{pp}$ range (V)
$H_2SO_4$	0.5	0.4108	0.0387	1.301-1.5341
HETPB	$1 \times 10^{-2}$	0.4032	-	-
	$7 \times 10^{-3}$	0.3822	-	-
	$4 \times 10^{-3}$	0.3439	0.0411	-
	$1 \times 10^{-3}$	0.3348	0.0090	0.6650-1.3190

When mild steel is exposed to 0.5 M  $H_2SO_4$ , there is a formation of passive layer and the same trend is obtained with lower concentration of inhibitor ( $1 \times 10^{-3}$  M) which indicates that film formed on

mild steel surface is adherent. The  $i_c$  values in Table 2 were found to be lower in presence of different concentrations of HETPB ( $1 \times 10^{-2}$  to  $1 \times 10^{-3}$ ) M as compared to  $H_2SO_4$ , which suggest that HETPB is getting adsorbed on the surface of metal thereby lowering the maximum current. Therefore, HETPB acts as a good corrosion inhibitor.

When mild steel exposed to higher concentrations of HETPB ( $1 \times 10^{-2}$  to  $4 \times 10^{-3}$ ) M no passivation range is observed. This indicates that HETPB at higher concentrations acts as non-passivating type of inhibitor for mild steel in 0.5 M  $H_2SO_4$ . This is because, corrosion products are either soluble or the film formed is not adherent.

### 3.3. Electrochemical Impedance Spectroscopy (EIS)

**Table 3.** Impedance parameters ( $R_{ct}$ ,  $f$  and  $C_{dl}$ ) and inhibition efficiency ( $I\%$ ) for the corrosion of mild steel in 0.5 M  $H_2SO_4$  without and with addition of various concentrations of HETPB at 298K.

Compound	Concentration (M)	$R_{ct}$ ( $\Omega cm^2$ )	$f$ (Hz)	$C_{dl}$ (F/cm <sup>2</sup> )	$I$ (%)
$H_2SO_4$	0.5	3.454	11.91	$3.164 \times 10^{-3}$	-
HETPB	$1 \times 10^{-2}$	479.317	5.486	$6.680 \times 10^{-5}$	99.28
	$7 \times 10^{-3}$	1792.078	19.766	$4.697 \times 10^{-6}$	99.81
	$4 \times 10^{-3}$	1326.400	1.738	$7.409 \times 10^{-5}$	99.74
	$1 \times 10^{-3}$	561.021	3.742	$8.184 \times 10^{-5}$	99.38

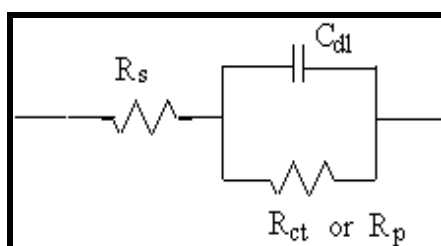
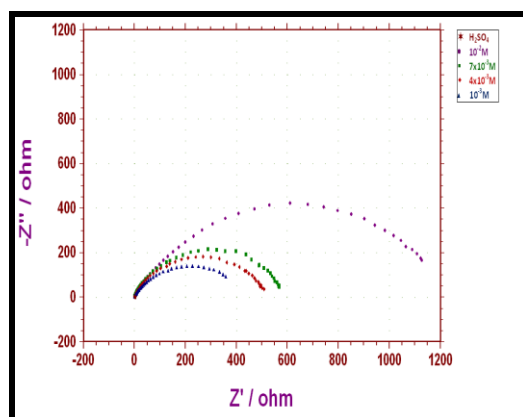
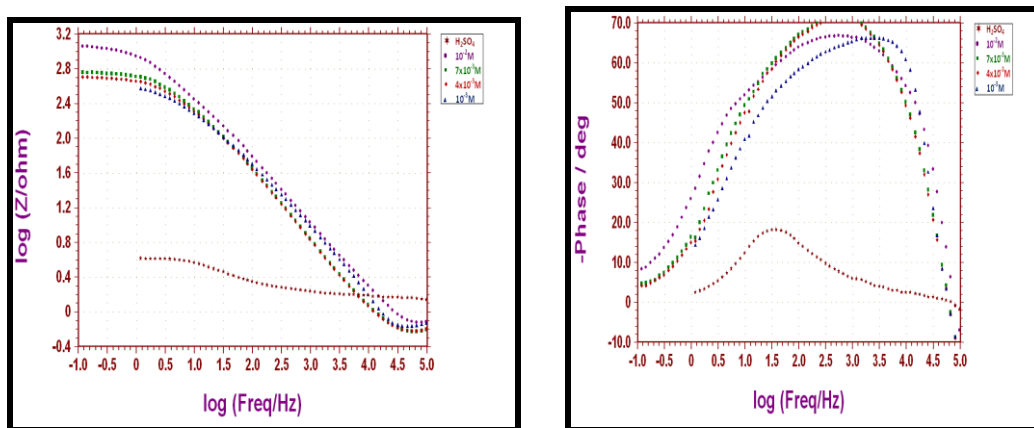


**Figure 4.** Equivalent circuit of the impedance spectra.



(a)



(b)

**Figure 5.** Nyquist plot (a) and Bode Plots (b) for mild steel in 0.5 M H<sub>2</sub>SO<sub>4</sub> solution in the absence and presence of various concentration of HETPB.

The corrosion of mild steel in acidic solution, in the presence of HETPB, was investigated by EIS at 298 K after immersion for 5hrs. Impedance parameters are given in Table 3 and the equivalent circuit diagram are given in Figure 4. Nyquist and Bode Plot are given in Figure 5(a) and 5(b).

Double layer capacitance values ( $C_{dl}$ ) and charge transfer resistance values ( $R_{ct}$ ) were obtained from impedance measurement. The value of charge transfer resistance was obtained measuring the diameter of the semicircle and the double layer capacitance was calculated using the following relation:

$$C_{dl} = (2\pi f R_{ct})^{-1}$$

The inhibition efficiency is also calculated using the equation given below:

$$I\% = \left( \frac{R_{ct(i)} - R_{ct(a)}}{R_{ct(i)}} \right) \times 100 \tag{2}$$

where  $R_{ct(a)}$  and  $R_{ct(i)}$  are charge transfer resistance values with and without inhibitor for mild steel in 0.5 M H<sub>2</sub>SO<sub>4</sub>.

Nyquist plots of mild steel in uninhibited solution (0.5 M H<sub>2</sub>SO<sub>4</sub>) displayed two capacitive loops. The high frequency (HF) loop i.e., the smaller one, can be attributed to the film formation at the steel surface while the low frequency (LF) loop i.e., the larger one, can be attributed to the charge transfer reaction. The HF capacitive loop is so small, that it cannot be seen clearly. HF loop indicates the existence of Warburg impedance [30] which is characteristic of the diffusion process (diffusion layer of finite thickness) [31]. The high frequency part of the impedance describes the behavior of inhomogeneous surface layer while the low frequency contribution shows the kinetic response for the charge transfer reaction. Nyquist plots of mild steel in inhibited acidic solutions containing ( $1 \times 10^{-2}$  to  $1 \times 10^{-3}$ ) M concentrations of HETPB displayed one capacitive arc as shown in Figure 5. It is apparent from Figure 5 that the impedance capacitive loop for mild steel in 0.5 M H<sub>2</sub>SO<sub>4</sub> solutions changes significantly with the increasing inhibitor concentrations. The diameter of the capacitor loop increases

tremendously in presence of inhibitor as compared to that of acid which indicates a high inhibition of corrosion. The largest capacitive loop was obtained for maximum concentration ( $1 \times 10^{-2}$  M) of inhibitor (HETPB).

Approximately semi-circular [32] appearance shown by impedance diagram indicates that corrosion of mild steel is mainly controlled by charge transfer process. AC impedance spectra have been used to detect the formation of the film formed on the metal surface. If the protective film is formed, the charges transfer resistance increases, and double layer capacitance value decreases [33]. The value of  $R_{ct}$  increases in the presence of inhibitor which in turn leads to a decrease in corrosion current for mild steel in 0.5 M  $H_2SO_4$ . All the concentrations of HETPB perform best in 0.5 M  $H_2SO_4$  by enhancing the value of  $R_{ct}$  and bringing down the  $C_{dl}$  value. This suggests that a protective film is formed on the metal surface of the metal. Higher values of  $R_{ct}$  which arise with all concentrations of HETPB as compared to  $R_{ct}$  value of acid, is indicative of greater inhibition efficiency. The double layer capacitance at the Fe/ $H_2SO_4$  interface decreases with an increase in inhibitor concentration. The results obtained by the impedance studies correlate very well with the potentiodynamic results for all the three concentrations of inhibitor at 298 K. The inhibition efficiencies show an extremely good quantitative correlation.

#### 3.4. Adsorption isotherm

**Table 4.** The value of surface coverage ( $\theta$ ) of mild steel in 0.5 M  $H_2SO_4$  in the presence of HETPB at different temperatures.

Temp. (K)	Concentration (M)	$i_{corr}$ ( $A/cm^2$ ) $\times 10^5$	I%	$\theta$
298	$1 \times 10^{-2}$	14.55	98.84	0.9884
	$7 \times 10^{-3}$	1.19	99.98	0.9998
	$4 \times 10^{-3}$	1.49	99.97	0.9997
	$1 \times 10^{-3}$	2.54	99.96	0.9996
	$H_2SO_4$	967.90	-	-
308	$1 \times 10^{-2}$	2.62	99.85	0.9985
	$7 \times 10^{-3}$	29.07	98.30	0.9830
	$4 \times 10^{-3}$	28.93	98.31	0.9831
	$1 \times 10^{-3}$	5.17	99.69	0.9969
	$H_2SO_4$	1712.00	-	-
318	$1 \times 10^{-2}$	21.93	98.88	0.9888
	$7 \times 10^{-3}$	10.12	99.48	0.9948
	$4 \times 10^{-3}$	35.13	98.20	0.9820
	$1 \times 10^{-3}$	567.30	70.97	0.7097
	$H_2SO_4$	1954.00	-	-
328	$1 \times 10^{-2}$	33.57	98.48	0.9848
	$7 \times 10^{-3}$	47.81	97.83	0.9783
	$4 \times 10^{-3}$	39.99	98.12	0.9812
	$1 \times 10^{-3}$	2022.00	8.46	0.0846
	$H_2SO_4$	2209.00	-	-

In order to gain more information about the mode of adsorption of these compounds on the surface of mild steel, the experimental data have been tested with several adsorption isotherms. The values of surface coverage ( $\theta$ ) is obtained by using equation below are given in Table 4.

$$\theta = I\%/100 \tag{3}$$

The surface coverage values ( $\theta$ ) were evaluated by using inhibition efficiency values obtained from potentiodynamic polarization studies.

Various isotherms were studied for the adsorption of HETPB on mild steel. On comparing the  $R^2$  values of various isotherms it is concluded that adsorption of HETPB on the mild steel in 0.5 M  $H_2SO_4$  follows Langmuir adsorption isotherm ( $R^2 = 0.9996$ ) and is given in Table 5.

**Table 5.** Slope (x), Intercept (c) and Correlation coefficient ( $R^2$ ) values of the curve between  $c/\theta$  versus c for HETPB.

Temp. (K)	Slope (x)	Intercept (c)	$R^2$
298	1.017	$3 \times 10^{-5}$	0.9999
308	1.003	$4 \times 10^{-5}$	0.9998
318	0.969	$3 \times 10^{-3}$	0.9999
328	0.994	$2 \times 10^{-3}$	0.9987

According to Langmuir’s adsorption isotherm [34-36], the surface coverage is related on the equilibrium constant  $K_{ads}$  and concentration of inhibitor c via ( $\theta$ ).

$$c/\theta = 1/K_{ads} + c \tag{4}$$

where  $c/\theta$  is plotted against c, it arises linearly to give intercept, which is equal to  $1/K$ , and slope of the line is unity and is given in Figure 6.

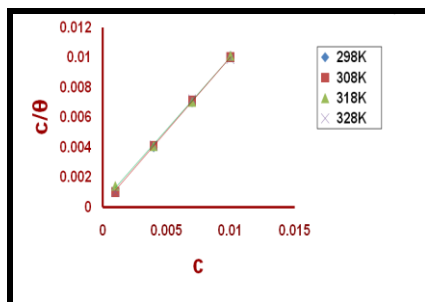


**Figure 6.** Langmuir isotherm for adsorption of HETPB on the mild steel surface.

The equilibrium constant adsorption process is related to the free energy of adsorption,  $\Delta G^{\circ}_{\text{ads}}$ , and is expressed by following equation given below:

$$K_{\text{ads}} = 1/55.5 \exp(-\Delta G^{\circ}_{\text{ads}}/RT) \quad (5)$$

where 55.5 is the molar concentration of water in the solution expressed in M ( $\text{molL}^{-1}$ ), R is the gas constant ( $8.314\text{JK}^{-1}\text{mol}^{-1}$ ) and T is the absolute temperature (K). The thermodynamics parameters derived from Langmuir adsorption isotherms for the studied compound are given in Table 6.

**Table 6.** Equilibrium constant (K) and Gibbs free energy ( $\Delta G^{\circ}_{\text{ads}}$ ) values for HETPB calculated from Langmuir adsorption isotherm.

Temp. (K)	Slope (x)	Intercept (c)	R <sup>2</sup>	K	$-\Delta G^{\circ}_{\text{ads}}$ (KJ/mol)
298	1.017	$3 \times 10^{-5}$	0.9999	33333	35.76
308	1.003	$4 \times 10^{-5}$	0.9998	25000	36.22
318	0.969	$3 \times 10^{-3}$	0.9999	3333	32.07
328	0.994	$2 \times 10^{-3}$	0.9987	5000	34.18

The negative values of  $\Delta G^{\circ}_{\text{ads}}$  along with the higher K values indicate a spontaneous adsorption process. Generally, the energy values of  $-20 \text{ kJmol}^{-1}$  or less negative are associated with an electrostatic interaction between charged molecules and charge metal surface, physisorption; those of  $-40 \text{ kJmol}^{-1}$  or involve more negative charge sharing or transfer from the inhibitor molecules to the metal surface to form a coordinate covalent bond, chemisorption [37]. The values of  $\Delta G^{\circ}_{\text{ads}}$  in our measurements range from  $(-32 \text{ to } -36) \text{ kJmol}^{-1}$  and are given in Table 6, it is suggested that adsorption of this phosphonium compound involves two types of interaction such as chemisorption and physisorption.

### 3.5. Kinetic studies

Effective activation energy is calculated using the equation given below:

$$\log i_{\text{corr}} = B - E_a / 2.303RT \quad (6)$$

Fig. 7 shows the graph between  $\log i_{\text{corr}}$  versus  $1/T$ . Effective activation energy values were calculated from the slope of these curves and are given in Table 7.

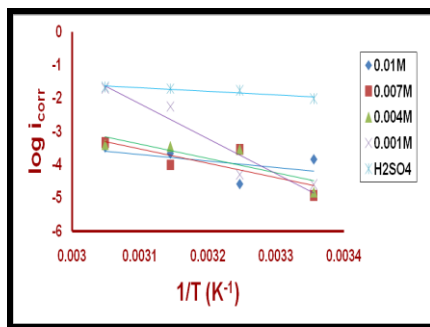


**Figure 7.** Plotting  $\ln i_{\text{corr}}$  vs.  $1/T$  to calculate the activation energy of corrosion process in the presence of inhibitor.

**Table 7.** Calculated values of effective activation energy ( $E_a$ ) for the corrosion of mild steel in 0.5 M  $\text{H}_2\text{SO}_4$  in the presence of HETPB at different concentrations.

Concentration (M)	$E_a$ (kJ/mol)
$\text{H}_2\text{SO}_4$	21.11
$1 \times 10^{-2}$	35.97
$7 \times 10^{-3}$	81.03
$4 \times 10^{-3}$	81.94
$1 \times 10^{-3}$	197.81

The effective activation energy for corrosion of mid steel in 0.5 M  $\text{H}_2\text{SO}_4$  was found to be 21.11kJ/mol. It can be seen from the Table 7, the activation energy ( $E_a$ ) of the corrosion of mild steel in 0.5 M  $\text{H}_2\text{SO}_4$  solution in the presence of HETPB was higher than that in the free acid solution which may be interpreted as physical adsorption mechanism [38, 39]. Hence, HETPB induces higher energy barrier and therefore the rate of corrosion decreases.

### 3.6. SEM Analysis

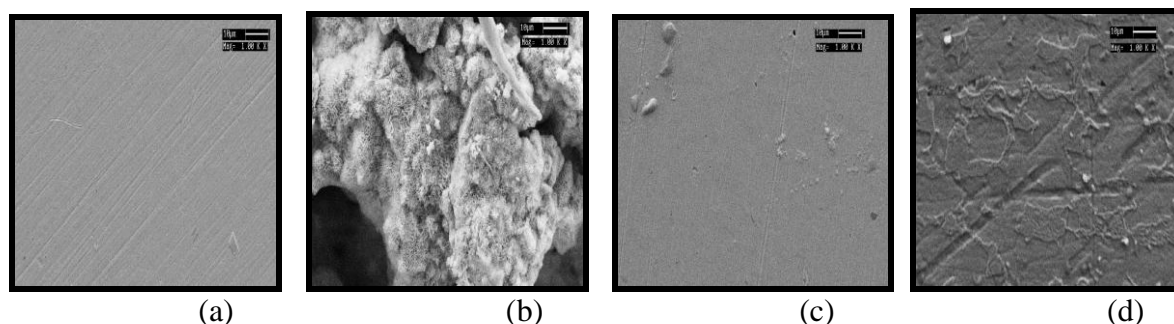


**Figure 8.** Scanning electron micrograph of: (a) plain mild steel surface, (b) 0.5M  $\text{H}_2\text{SO}_4$ , (c)  $1 \times 10^{-2}$  M HETPB and (d)  $1 \times 10^{-3}$  M HETPB at 1000 magnifications.

SEM micrographs were obtained from mild steel surface specimens after immersion in 0.5 M  $\text{H}_2\text{SO}_4$  solutions for 12 h in the absence and presence of  $1 \times 10^{-2}$  and  $1 \times 10^{-3}$  M of HETPB, are shown in Figure 8 (a), 8(b), 8(c) and 8(d).

It can be observed from Figure 8(b) that the specimen surface was strongly damaged in the absence of the inhibitor. It can be seen from Figure 8(c) that at higher concentration of inhibitor that is  $1 \times 10^{-2}$  M HETPB, the metal surface is fully covered with the inhibitor molecules giving it a high degree of protection against corrosion. Figure 8(d) shows that at lowest concentration of inhibitor, that is,  $1 \times 10^{-3}$  M the metal surface is covered with corrosion products. But the extent of corrosion in the presence of inhibitor is much less compared to specimens exposed to 0.5 M sulfuric acid shown by Figures 8(c) and 8(d).

### 3.7. Atomic Force Microscopy

Atomic Force Microscopy is a method of measuring surface shape and topography on a scale from angstroms to 100 microns. In the present work, average area analysis method is employed to calculate the roughness of metal surface. In this average area analysis, whole area of one side of metal surface was considered. Topographical changes were qualitatively characterized by AFM images which are given in Figures 9(a), 9(b), 9(c) and 9(d).

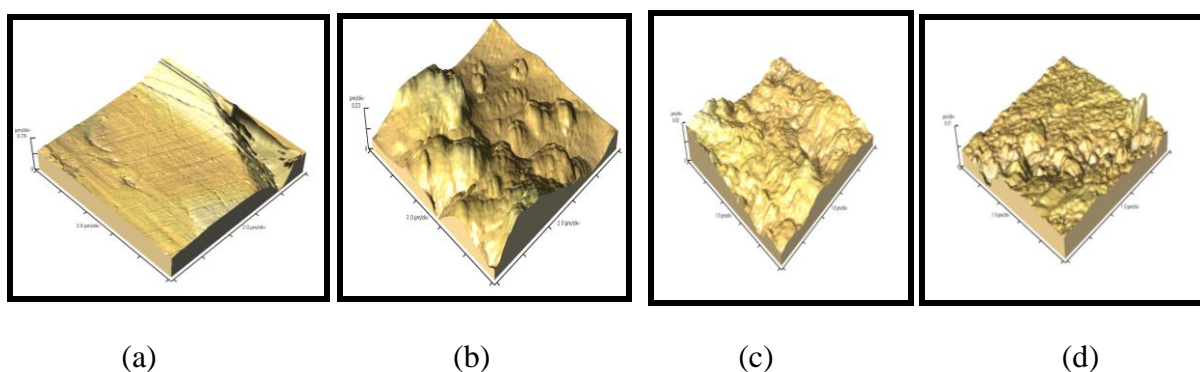


**Figure 9.** Atomic force micrograph of: (a) plain mild steel surface, (b) 0.5M  $\text{H}_2\text{SO}_4$ , (c)  $1 \times 10^{-2}$  M HETPB and (d)  $1 \times 10^{-3}$  M HETPB at 1000 magnifications.

Figure 9(a) shows the atomic force micrograph of plain mild steel specimen whereas Figure 9(b) shows the atomic force micrograph of mild steel specimen dipped in 0.5 M  $\text{H}_2\text{SO}_4$  solution. The atomic force micrographs of mild steel specimen dipped in  $1 \times 10^{-2}$  M HETPB and  $1 \times 10^{-3}$  M HETPB are shown in Figures 9(c) and 9(d). The surface morphology of the plain mild steel indicates that there were a few scratches from the mechanical polishing treatment. The mild steel surface was corroded when exposed to  $\text{H}_2\text{SO}_4$ . This can be qualitatively seen from AFM micrographs as there is a formation of deep holes and pits.

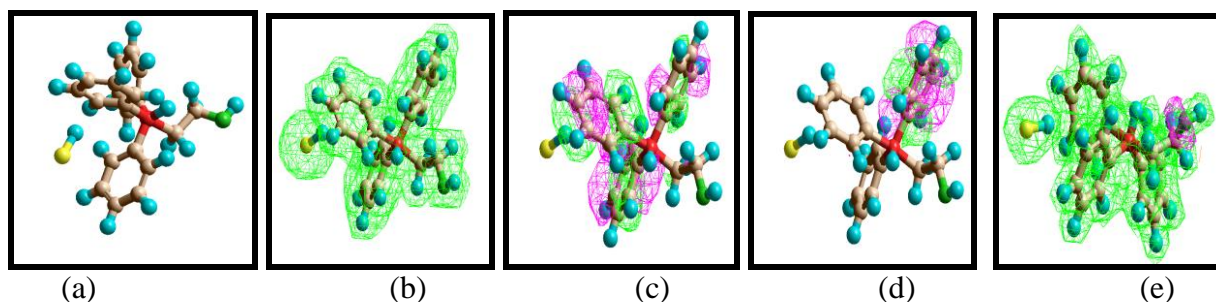
**Table 8.** Roughness of Metal surface from Atomic Force micrographs.

Compound	Concentration (M)	Average area RMS(nm)
H <sub>2</sub> SO <sub>4</sub>	0.5	503.2
HETPB	1×10 <sup>-2</sup>	118.7
	1×10 <sup>-3</sup>	200.9

The metal surface could be quantitatively evaluated by measuring the change in the surface roughness (RMS). RMS value signifies the extent of corrosion i.e. higher the RMS value more will be the extent of corrosion. The RMS value of mild steel dipped in 0.5 M H<sub>2</sub>SO<sub>4</sub> was obtained 503.2nm. The RMS values were obtained 118.7 nm and 200.9 nm for mild steel dipped in 1×10<sup>-2</sup> M and 1×10<sup>-3</sup> M of inhibitor and are given in Table 8. This indicates that extent of corrosion is maximum in presence of acid and extent of corrosion is least for maximum concentration of inhibitor which is 1×10<sup>-2</sup> M.

### 3.8. Quantum Chemical Analysis

Through these calculations, an attempt has been made to correlate corrosion inhibition efficiency (dependent variable) with the set of some independent variables like energy of HOMO, LUMO, and dipole moment etc. The optimized geometry of this is given in Figures 10(a), 10(b), 10(c), 10(d) and 10(e). The various optimized PM3 parameters for this additive are given in Table 9.

**Figure 10.** Optimized structures of the HETPB (a-d).**Table 9.** Optimized AM1 parameters for the inhibitors using Hyperchem 7.5.

Inhibitors	Binding Energy (kcal/mol)	Heat of Formation (kcal/mol)	E <sub>HOMO</sub> (eV)	E <sub>LUMO</sub> (eV)	Dipole Moment (Debye)	E <sub>LUMO</sub> -E <sub>HOMO</sub>
HETPB	-4700.59	-25.31	-9.58	0.18	3.18	9.76

The binding energy of HETPB is found to be negative which suggests that HETPB is very stable inhibitor molecule and less prone to be split apart. The heat of formation of this molecule is negative which suggests that the formation of this molecule is spontaneous and it is stable. HETPB has the negative charge cloud which is available for the donation to the metal surface. Dipole moment

values provide information about the inhibition efficiency. Higher the value of dipole moment, higher is the extent of polarization, and greater is the tendency of donation of electrons to the metal surface. The inhibition energy increases with increasing values of  $E_{\text{HOMO}}$  and decreasing values of  $E_{\text{LUMO}}$ . In the present investigation, no co-relation is found between the values of HOMO, LUMO and the energy gap of HOMO and LUMO and experimental inhibition efficiencies. This is due to non-planarity of the inhibitor molecule and extent of delocalization, which causes steric hindrance in adsorption on the metal surface or it may be due to the complex interaction in adsorption process, both chemisorption and physisorption might take place, the conclusion is in agreement with the result of  $\Delta G_{\text{ads}}^{\circ}$  which was obtained from the thermodynamics calculations.

#### 4. CONCLUSIONS

The goal of this research is to investigate the inhibition action of HETPB on the corrosion of mild steel in 0.5 M  $\text{H}_2\text{SO}_4$  at (298 to 328) K. The results show that HETPB is an excellent inhibitor with inhibition efficiency from 99% to 90% for mild steel in 0.5 M  $\text{H}_2\text{SO}_4$ . The  $E_{\text{corr}}$  values remains constant indicating that HETPB is mixed type of inhibitor in 0.5 M  $\text{H}_2\text{SO}_4$  i.e., blocking both cathodic and anodic reactions to an equal extent. The irregular trends of  $b_c$  and  $b_a$  values indicates that adsorption of HETPB may have the involvement of other species/anions present in the solution. The values of  $b_a$  which is greater than  $b_c$  indicate that corrosion process is taking place by blocking anodic dissolution process. This indicates that HETPB predominantly acts as anodic type of inhibitor. Adsorption of HETPB on the mild steel follows Langmuir adsorption isotherm. The negative values of  $\Delta G_{\text{ads}}^{\circ}$  indicate the spontaneity of the adsorption process.  $\Delta G_{\text{ads}}^{\circ}$  almost remains constant with temperature in the case of HETPB. The values of  $E_a$  in presence of HETPB are higher as compared to the pure acid. Although there is a decrease in  $i_c$  value as compare to the acid but no passivation range is observed for higher concentrations of HETPB. This indicates that HETPB acts as non-passivating type of inhibitor for mild steel in 0.5 M  $\text{H}_2\text{SO}_4$  at a higher concentration and at lower concentrations it behaves as a passivating type of inhibitor. The diameter of the capacitor loop increases tremendously in presence of HETPB as compared to that of the acid which indicates a high inhibition of corrosion. The value of  $R_{\text{ct}}$  (charge transfer resistance) increases in the presence of inhibitor which in turn leads to a decrease in corrosion current for mild steel in 0.5 M  $\text{H}_2\text{SO}_4$ . The  $C_{\text{dl}}$  double layer capacitance value shows a decrease on the addition of inhibitor as compared to that of the acid, indicating a complete film formation on the metal surface in the presence of the inhibitor. Surface morphology study (SEM) reveals that the extent of corrosion inhibition is more at higher concentration as compared to the lower concentration. Decrease in RMS value in presence of inhibitor shows that HETPB is a good corrosion inhibitor. Results obtained from various techniques supplement each other.

#### ACKNOWLEDGEMENTS

The authors acknowledge University of Delhi for providing financial assistance and University of KwaZulu-Natal for a postdoctoral scholarship for Dr I. Bahadur.

#### References

1. O.K. Abiola, J.O.E. Otaigbe, O.J. Kio, *Gossipium hirsutum.*, *Corrosion Science* 51 (2009) 1879–1881.

2. D. Mercier, M.-G. Barthés-Labrousse, *Corrosion Science* 51 (2009) 339–348.
3. K.C. Emergul, A.A. Aksut, *Corrosion Science* 42 (2000) 2051–2067.
4. J. Zhang, M. Klasky, B.C. Letellier, *Journal of Nuclear Materials* 384 (2009) 175–189.
5. A.A. El-Shafei, S.A. Abd El-Maksoud, A.S. Fouda, *Corrosion Science* 46 (2004) 579–590.
6. A.I. Onuchukwu, *Materials Chemistry and Physics* 24 (1990) 337–341.
7. S.I. Pyun, S.-M. Moon, S.-H. Ahn, S.-S. Kim, *Corrosion Science* 41 (1999) 653–667.
8. L. Gnana Sahaya Rosilda, M. Ganesan, M. Anbu Kulandainathan, V. Kapali, *Journal of Power Sources* 50 (1994) 321–329.
9. M. Saleh, A.A. Ismail, A.A. El Hosary, *Corrosion Science* 23 (1983) 1239–1241.
10. M. Krishnan, N. Subramanyan, *Corrosion Science* 17 (1977) 893–900.
11. H.B. Shao, J.M. Wang, Z. Zhang, J.Q. Zhang, C.N. Cao, *Materials Chemistry and Physics* 77 (2002) 305–309.
12. I. Sekine, Y. Nakahata, H. Tanabe, The corrosion, *Corrosion Science* 28 (1988) 987.
13. E.E. Oguzie, R.N. Okolue, C.E. Ogukwe, C. Unaegbu, *Materials Letters* 60 (2006) 3376–3378.
14. S.A. Ali, M.T. Saeed, S.V. Rahman, *Corrosion Science* 45 (2003) 253–266.
15. M. Lagrenee, B. Mernari, M. Bouanis, M. Traisnel, F. Bentiss, *Corrosion Science* 44(2002) 573–588.
16. M.A. Mighahed, *Material Chemistry & Physics*, 93 (2005) 48-53.
17. M.A. Quraishi, M. Athar, H. Ali, *British Corrosion Journal* 37 (2002) 155–158.
18. J. Cruz, R. Martinez, J. Genesca, E.G. Ochoa, *Journal of Electroanalytical Chemistry*, 566 (2004) 111-121.
19. M.A. Quraishi, S. Khan, *Journal of Applied Electrochemistry* 36 (2006) 539–544.
20. K.C. Emergul, Atakol, *Material Chemistry & Physics* 82 (2003) 188.
21. S.N. Raicheva, B.V. Aleksiev, E.I. Sokolova, *Corrosion Science* 34 (1993) 343.
22. S. Arab, E.A. Noor, *Corrosion* 49 (2) (1993) 122.
23. A. Sayed El, *Journal of Applied Electrochemistry* 27 (1997) 193.
24. X.L. Cheng, H.Y. Ma, S. Chen, R. Yu, X. Chen, Z.M. Yao, *Corrosion Science* 41 (1993) 321.
25. S.S. Abd, El Rehim, M.A.M. Ybrahim, K.F. Khalid, *Journal of Applied Electrochemistry* 29 (1999) 593.
26. K. Bhrara, H. Kim, G. Singh, *Corrosion Science* 50 (2008) 2747-2754.
27. A. Nahle, I. Abu-Abdoun, I. Abdel-Rahman, *Anti-Corrosion Methods and Materials* 55 (2008) 217-224.
28. M. Sharma, G. Singh, *International Journal of Chemistry and Applications* 5 (2013) 13-25.
29. G. Moratti, F. Guidi, F. Fabris, *Corrosion Science* 76 (2013) 206-218.
30. W. Warburg, *Ann. Phys* 6 (1901) 125.
31. C. Gabrielli, in: *Identification of Electrochemical Processes by Frequency Response Analysis*, Solartron, Franborough, UK, 1980, p. 62.
32. F. Bentiss, M. Traisenl, M. Lagrenee, *Corrosion Science*, 42 (2000) 127-146.
33. K. C. Emergul, E. Duzgun, O. Atakol, *Corrosion Science*, 48 (2006) 3243-3260.
34. V.R. Saliyan, A.V. Adikari, *Corrosion Science* 50 (2008) 55-61.
35. S. K. Shukla, M.A. Quarishi, *Corrosion Science* 51 (2009) 1990-1997.
36. K.C. Emergul, O. Atakol, *Material Chemistry & Physics* 83 (2004) 373-379.
37. M. Behpour, S.M. Ghoreishi, N. Soltani, M. Salavati-Niasari, M. Hamadani, A. Gandomi, *Corrosion Science* 50 (2008) 2172-2181.
38. E.E. Oguzie, *Corrosion Science* 50 (2008) 2993–2998.
39. A. Popova, E. Sokolova, S. Raicheva, M. Christov, *Corrosion Science* 45 (2003) 33–58.